SorLA regulates the activity of lipoprotein lipase by intracellular trafficking

Stine C. Klinger[1], Simon Glerup[1], Merete K. Raarup[2], Muriel C. Mari[3], Mette Nyegaard[4], Gerbrand Koster[5], Thaneas Prabakaran[1], Stefan K. Nilsson[6], Maj M. Kjaergaard[2], Oddmund Bakke[5], Anders Nykjær[1], Gunilla Olivecrona[6], Claus Munck Petersen[1] and Morten S. Nielsen[1,*]

[1]The MIND-Center, Department of Medical Biochemistry, University of Aarhus, Ole Worms Allé 1170, DK 8000 Aarhus C, Denmark
[2]The MIND-Center, Stereology and Electron Microscopy Research Laboratory, University of Aarhus, Ole Worms Allé 1185, DK 8000, Aarhus C, Denmark
[3]Department of Cell Biology, UMCU, Utrecht, AZU, Heidelberglaan 100, 3584 CX Utrecht, The Netherlands
[4]Department of Haematology, Aalborg Hospital, Mølleparkvej 4, Postboks 561, 9100 Aalborg, Denmark
[5]Department of Molecular Biosciences, University of Oslo, Postbox 1041 Blindern, N-0316 Oslo, Norway
[6]Department of Medical Biosciences, Umea University, SE-901 87 Umeå, Sweden
*Author for correspondence (mn@biokemi.au.dk)

Accepted 6 October 2010
Journal of Cell Science 124, 1095-1105

doi:10.1242/jcs.072538

Summary

Many different tissues and cell types exhibit regulated secretion of lipoprotein lipase (LPL). However, the sorting of LPL in the trans Golgi network has not, hitherto, been understood in detail. Here, we characterize the role of SorLA (officially known as SorLA-1 or sortilin-related receptor) in the intracellular trafficking of LPL. We found that LPL bound to SorLA under neutral and acidic conditions, and in cells this binding mainly occurred in vesicular structures. SorLA expression changed the subcellular distribution of LPL so it became more concentrated in endosomes. From the endosomes, LPL was further routed to the lysosomes, which resulted in a degradation of newly synthesized LPL. Consequently, an 80% reduction of LPL activity was observed in cells that expressed SorLA. By analogy, SorLA regulated the vesicle-like localization of LPL in primary neuronal cells. Thus, LPL binds to SorLA in the biosynthetic pathway and is subsequently transported to endosomes. As a result of this SorLA mediated-transport, newly synthesized LPL can be routed into specialized vesicles and eventually sent to degradation, and its activity thereby regulated.

Key words: Intracellular trafficking, Lipoprotein lipase, SorLA (SORL1), Vps10p-domain receptor

Introduction

SorLA (sortilin-related receptor; also known as and hereafter referred to as SorLA), sortilin and SorCS1, SorCS2 and SorCS3 constitute the mammalian Vps10p-domain (Vps10p-D) receptor family. The common feature of this receptor family is the luminal Vps10p-D, which is dominated by a large ligand-binding ten-bladed β-propeller (Mazella et al., 1998; Petersen et al., 1997; Quistgaard et al., 2009). In addition to the Vps10p-D, the luminal parts of SorCS1, 2 and 3 also have short leucine-rich sequences (Hermey et al., 2004). SorLA is the largest Vps10p-D receptor and is far more complex. Apart from the Vps10p-D, the most prominent structural elements of SorLA are the 11 low-density lipoprotein (LDL)-receptor class A (LA) repeats and a β-propeller domain known from the LDL receptor family (Jacobsen et al., 1996). SorLA is therefore also known as LDL receptor 11 (LR11) (Yamazaki et al., 1997). The Vps10p-D carries a propeptide that is removed in the late trans Golgi network (TGN) by the proprotein convertase furin (Munck Petersen et al., 1999). Although ligand binding to the Vps10p-D in both sortilin and SorLA is impaired by the propeptide, binding of ligands to the LA repeats in SorLA is not affected (Westergaard et al., 2004). Sortilin and SorLA are multi-ligand-binding receptors, and their Vps10p domains are targeted by several growth factors and peptides. In addition, the LA repeats of SorLA interact with, for example, components of the plasminogen-activating system, platelet-derived growth factor, receptor-associated protein (RAP), apolipoprotein E and apolipoprotein AV (Gliemann et al., 2004; Jacobsen et al., 1996; Nilsson et al., 2008; Nilsson et al., 2007). SorLA is expressed at substantial levels in many tissues, such as kidney, testis, ovary, lymph nodes, vascular smooth muscle cells (SMCs) and in various parts of the nervous system.

Sortilin and SorLA are multifunctional receptors, and they both mediate endocytic activity and trafficking among intracellular vesicles. For instance, we have shown that sortilin and SorLA shuttles between the TGN and late endosomes (Nielsen et al., 2007; Nielsen et al., 2001). This type of trafficking involves interactions between the cytoplasmic domain of the receptors and various adaptors, including adaptor-protein-1 (AP1), Golgi-localized, γ ear-containing, ARF-binding proteins (GGA1, GGA2 and GGA3) and the retromer complex (Nielsen et al., 2007). One known function of SorLA is to protect the amyloid precursor protein (APP) from proteolysis into soluble APPβ and the insoluble amyloid β-peptide (Aβ) (Rogaeva et al., 2007). In fact, SorLA has been genetically associated with late-onset Alzheimer's disease (Andersen et al., 2005). SorLA has a different role in the vascular system, where a secreted soluble form of SorLA enhances intimal migration of SMCs, by interaction with urokinase-type plasminogen activator receptor (Gliemann et al., 2004; Ohwaki et al., 2007).

Lipoprotein lipase (LPL) is differentially expressed in adipose tissue, heart and skeletal muscles cells, macrophages, the mammary gland, regions of the nervous system and in several other tissues (Braun and Severson, 1992). LPL hydrolyzes triacylglycerols in circulating lipoproteins, but can also function as a bridging molecule

Journal of Cell Science

between lipoproteins and cellular membrane receptors or heparan sulfate proteoglycans. In the brain, LPL is believed to be involved in synaptic remodeling following injury by transporting cholesterol and lipids (Blain et al., 2004; Paradis et al., 2004). Newly synthesized LPL is glycosylated and assembled into a homodimer in the endoplasmic reticulum (ER), where the enzyme also obtains its catalytic activity by a lipase maturation factor 1 (LMF1)-dependent process (Peterfy et al., 2007). After passing through the Golgi network, LPL is secreted, accumulated in vesicles or sent to lysosomes for degradation (Cupp et al., 1987; Vannier and Ailhaud, 1989). Many physiological conditions are known to affect LPL activity by post-translational mechanisms. As an example, LPL activity is rapidly downregulated during fasting in adipose tissue, by a mechanism that is independent of the level of *LPL* mRNA (Bergo et al., 2002). Although the transcriptional control of LPL has been well described, the post-translational mechanisms regulating the level of secreted active LPL in several physiological states are far from understood (Preiss-Landl et al., 2002; Wang and Eckel, 2009).

As SorLA is engaged in intracellular trafficking, we have examined the influence of SorLA on the intracellular sorting and turnover of LPL. We demonstrate that SorLA binds LPL in intracellular vesicles and mediates a more vesicular localization of LPL in transfected cells, as well as in primary neuronal and glial cultures. Moreover, we show that SorLA mediates a direct transport of LPL from the TGN to the endosomes, from which LPL is delivered to the lysosomes for degradation. Through this transport mechanism, SorLA is a post-translational regulator of LPL activity.

Results

The C-terminal domain of LPL binds to the LA repeats in SorLA

We have previously shown that LPL binds to sortilin with a high affinity though basic amino acids that are located in C-terminal folding domain of LPL (Nielsen et al., 1999). By using surface plasmon resonance (SPR) analysis, we also found a similar high affinity (25 nM) binding between LPL and SorLA (Fig. 1A). The neuropeptide neurotensin and RAP bind, respectively, to the Vps10p-D and the LA repeats in SorLA. As previously reported, we observed a complete inhibition of the binding between LPL and sortilin in the presence of neurotensin, whereas neurotensin had no effect on the interaction between LPL and SorLA (Fig. 1B). Likewise, we found LPL did not bind to the Vps10p domain of SorLA, indicating that LPL binds to the LA repeats in the luminal domain (Fig. 1A). Accordingly we found almost complete inhibition of the binding between LPL and SorLA in the presence of RAP (Fig. 1C). SPR analysis also mapped the receptor-binding site in LPL to the monomeric C-terminal folding domain, and demonstrated that both monomeric and dimeric LPL interact with SorLA (Fig. 1D). Finally, binding between LPL and SorLA was observed under slightly acidic conditions, like those that are found in the TGN and endosomes (Fig. 1E).

The intracellular localization of LPL is affected by SorLA expression

To characterize the functional impact of binding between LPL and SorLA, we stably transfected LPL into human embryonic kidney (HEK)-293 cells using the Invitrogen Flip-In system. Subsequently,

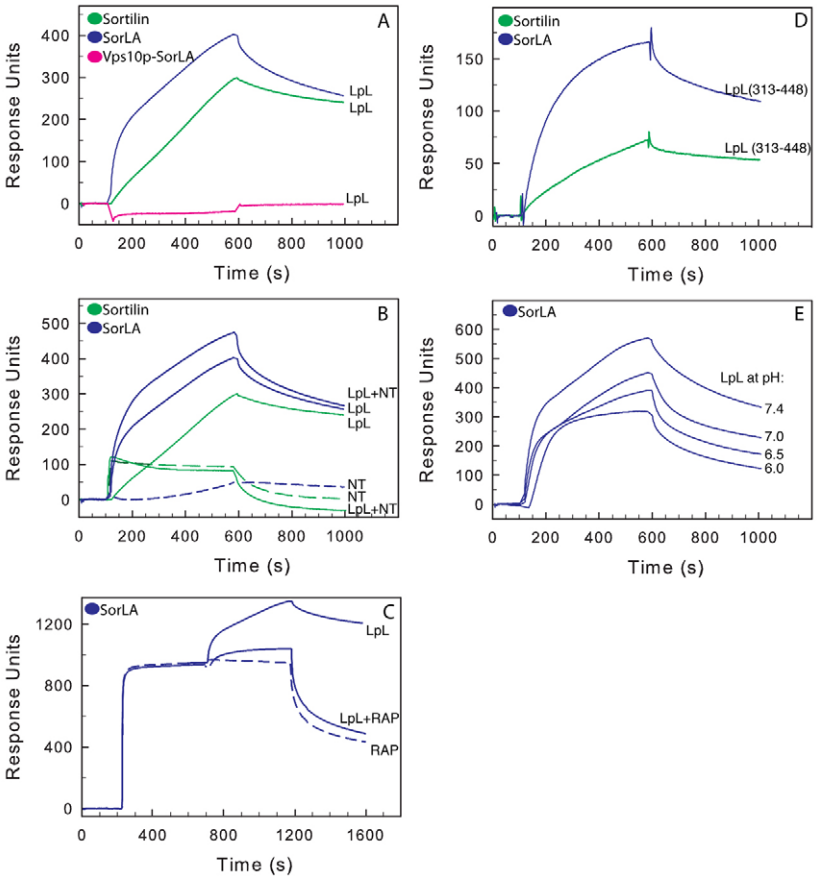

Fig. 1. Surface plasmon resonance analysis of binding of LPL to SorLA, Vps10p-D-SorLA and sortilin. Sensor chips were coupled covalently with SorLA (blue curves), sortilin (green curves) and the Vps10p-D of SorLA (magenta curves). The diagrams display the binding of 400 nM bovine LPL to the receptors (**A**) before or (**B**) after injection of 10 µM neurotensin (NT) and (**E**) at different pHs. (**C**) Inhibition of LPL binding to SorLA by RAP. SorLA was saturated with RAP (at 5 µM). After 600 seconds a mixture of RAP (5 µM) plus LPL (400 nM), or RAP (5 µM) alone, was coinjected. For comparison, the response obtained with LPL alone has been shifted to the level of RAP saturation. (**D**) 500 nM of the C-terminal folding domain in LPL {GST–LpL(313–488 del [390–393])} was used to map the binding domain. All perfusions were continued with buffer alone at 600 seconds (A, B, D and E) or at 1200 seconds (C).

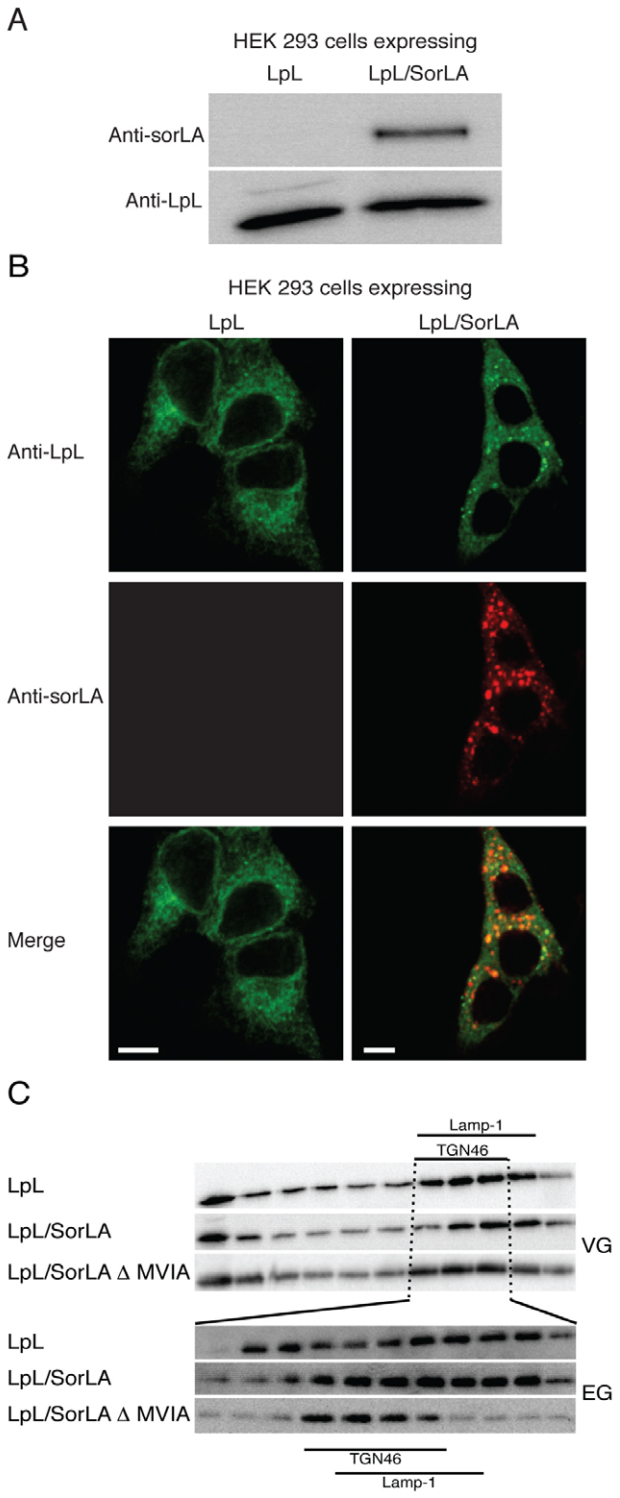

Fig. 2. The intracellular localization of LPL in stably transfected HEK-293 cells. (**A**) A western blot of 25 µg of total cell lysate, demonstrating the presence of LPL and SorLA in stably transfected cells (LpL/SorLA, cells cotransfected with LPL and SorLA). (**B**) Cells were fixed and stained with chicken anti-LPL antibody (green) or mouse anti-SorLA antibody (red). (**C**) Subcellular fractionation of transfected cells. Fractions 7–9 of the velocity gradient (VG) were subjected to equilibrium-gradient centrifugation (EG). Fractions were analyzed by western blotting with the mouse anti-LPL antibody. The fractions containing the indicated intracellular markers are marked by the bars. Scale bars: 5 µm.

this cell line was stably transfected with mutated or wild-type SorLA, or sortilin. Western blotting confirmed the presence of expressed LPL and SorLA in the transfected cells (Fig. 2A). Furthermore, quantitative real-time PCR (qRT-PCR) of *LPL* mRNA verified that expression of *LPL* was similar in SorLA- and sortilin-expressing and non-expressing HEK-293 cell lines, and was not affected by clonal selection (Table 1).

Immunofluorescent staining of LPL indicated that SorLA affects its overall cellular localization. LPL showed a strongly increased vesicular localization in cells expressing SorLA, whereas a less-disperse and perinuclear LPL localization was observed in cells expressing only LPL (Fig. 2B). To evaluate the increased vesicular staining observed by immunofluorescence, automated quantification of vesicular structures in LPL-transfected, and LPL and SorLA co-transfected, cells was performed using an Olympus scan^R imaging station. Before fixation, 20 units of heparin/ml was added to the medium, as it is well-known that heparin causes release of active LPL from the cell surface and thereby prevents any cellular uptake of LPL (Makoveichuk et al., 2004). As the cells are about 4-µm high and the LPL vesicles are distributed throughout the cell, a maximal intensity projection of a *z*-stack of four layers (1 µm apart) was used for quantification for each of the 121 recorded positions. We found 23.8 LPL-positive vesicles (s.e.±0.82, n=1580) in SorLA transfectants, but only 12.02 (s.e.±0.62, n=1054) in cells without SorLA, demonstrating a significantly higher amount of vesicular LPL in the presence of SorLA (P<0.0001) (see the Materials and Methods section for further description).

The changed subcellular localization of LPL in the presence of SorLA was also observed by using subcellular fractionation. After size separation in a velocity gradient (fractionated into 11 fractions), TGN46- and LAMP1-positive fractions (fractions 7–9) were separated further, according to buoyant density, by equilibrium gradient centrifugation. LPL was mainly concentrated in fractions 2–3 and 7–10 in LPL-expressing cells, but peaked in fractions 4–10 when coexpressed with SorLA (Fig. 2C). A changed subcellular pattern was also seen upon co-transfection of a LPL-expressing construct with a construct expressing a SorLA variant that exhibits impaired sorting due to a C-terminal truncation [SorLA-ΔMVIA; the MVIA motif mediates binding to the three GGA adaptors, and it was recently demonstrated that this interaction is involved in the TGN-to-endosome sorting of SorLA (Jacobsen et al., 2002; Nielsen et al., 2007)].

Intracellular localization of SorLA and LPL

The nature of the SorLA-positive vesicles was analyzed by immunoelectron microscopy. As expected, we mainly found SorLA staining in the ER, Golgi and endosomes, but occasionally we also

Table 1. Relative mRNA expression levels of *LPL* and *SORL1* in transfected cell lines

	Relative RNA expression (fold change)	
Cell line	*LPL*	*SORL1*
LPL	0.97±0.03	0.003±0.0008
LPL plus SorLA	0.91±0.26	1.00±0.43
LPL plus SorLA-ΔMVIA	1.02±0.20	1.18±0.31
LPL plus sortilin	0.98±0.05	0.002±0.0002

The endogenous housekeeping gene *HPRT1* was used to normalize for the number of cells. The mean expression levels (±s.d.) for each cell line were calculated from four biological quadruplicates (n=4).

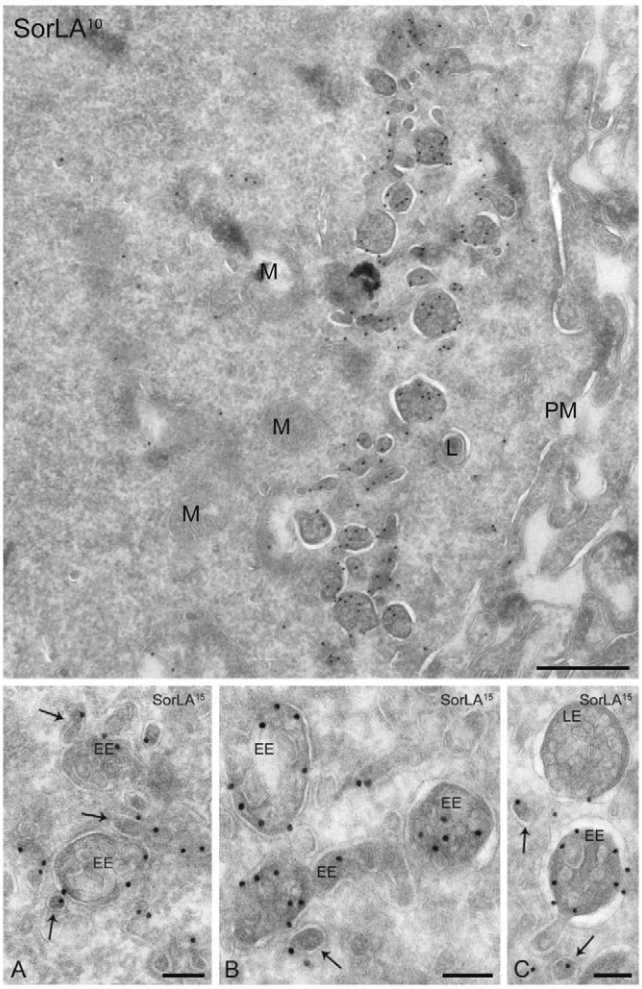

Fig. 3. Electron microscopy of SorLA intracellular localization. Ultrathin cryosections of HEK-293 SorLA cells were immuno-gold-labeled with the mouse anti-SorLA antibody. The gold size used for the immuno-labeling is indicated by the superscript number. The upper panel shows an overview of SorLA labeling in transfected HEK-293 cells. SorLA staining is primarily found in the Golgi and endosomes. The lower panels show enlarged pictures of endosomes. EEs and MVB/LEs have been defined as described previously (Mari et al., 2008). SorLA is found in the limiting membrane and inside EEs and late endosomes (LE), and in dense tubular structures in close vicinity to EEs (arrows). Scale bars: 100 nm. L, lysosomes; M, mitochondria; PM, plasma membrane.

found staining on the plasma membrane (Fig. 3, top panel). To differentiate between early endosomes (EEs) and multi-vesicular bodies/late endosomes (MVB/LEs), we use the definition described by Mari and colleagues in which endosomes with up to eight intraluminal vesicles are defined as EEs, whereas endosomes with nine or more intraluminal vesicles are defined as MVB/LEs (Mari et al., 2008). According to this definition, we observed intense staining of SorLA in MVB/LEs and, probably, also in EEs, represented by endosomes with fewer than nine intraluminal vesicles (Fig. 3, lower panel). However, as electron-dense tubules or vesicles are known to preferentially surround EEs, labeling in vesicles surrounded by these structures supports the presence of SorLA in EEs (arrows Fig. 3). Moreover, the SorLA-positive electron-dense tubules or vesicles resemble the endosome-to-TGN recycling compartments that are positive for sortilin, mannose-6-phosphate receptor (MPR) and sorting nexin-1 (SNX1), as described previously (Mari et al., 2008). As we did not succeed in acquiring electron microscope images of LPL, the presence of LPL in SorLA-positive vesicles was probed with fluorescence and crosslinking experiments.

Fluorescence studies show a punctated colocalization of LPL and SorLA in the cytoplasm (Fig. 4A). This observation was verified by use of a proximity ligation assay (PLA) that is based on antibodies tagged with circular DNA probes. Probes located less than 40 nm from each other can hybridize and subsequently be amplified with a polymerase (Soderberg et al., 2006). Interacting probes can be detected when fluorescently labeled oligonucleotides are used. Although this technique is not suitable for subcellular localization studies, Fig. 4B shows positive punctated staining in LPL and SorLA co-transfected cells, representing structures with SorLA and LPL in close proximity. For comparison, PLA using the same probes resulted in almost zero background in LPL-expressing cells devoid of SorLA (Fig. 4B, middle panel). To control for the specificity of this method, we also performed this experiment with an antibody against MPR300, which colocalizes with SorLA in the TGN. As we observed no positive interaction using PLA with anti-MPR300 and anti-LPL primary antibodies (Fig. 4B, right-hand panel), we conclude that LPL and SorLA are tightly colocalized.

Finally, in biolabeled HEK-293 cells expressing LPL or coexpressing LPL and SorLA, cellular proteins were crosslinked with the membrane-permeable cleavable crosslinker DSP [dithiobis(succinimidyl propionate)]. The 55-kDa LPL protein was precipitated using a rabbit anti-LPL antibody. In cells expressing SorLA, a 250-kDa protein, which corresponds to the size of SorLA, was co-precipitated with LPL (Fig. 4C, lane 4). Other, but much weaker, bands were present on the gel and might represent traces of dimerized LPL as well as traces of nonspecific protein interactions. No substantial bands were obtained after precipitation with beads without antibodies (Fig. 4C, lanes 1 and 3). Although the 250-kDa band was only present in cells expressing SorLA, and not in cells expressing only LPL, we confirmed further that the 250-kDa band represented SorLA by precipitating with an anti-SorLA antibody (Fig. 4D, top panel). As a negative control for nonspecific crosslinking between SorLA and other proteins in the biosynthetic pathway, crosslinked cell lysate from LPL and SorLA co-transfectants was immunoprecipitated with LMF1. This protein was mainly located in the ER, and did not result in SorLA precipitation (Fig. 4D, lower panel).

From these fluorescence and crosslinking experiments, we conclude that intracellular LPL and SorLA colocalize and that there is probably a physical interaction between these two proteins.

LPL is directly routed from the TGN to endosomes

We have previously reported that SorLA can reach endosomes either by retrograde trafficking from the cell surface or by direct transport from the TGN (Nielsen et al., 2007). To clarify whether LPL is transported directly to endosomes from the TGN, we first blocked protein synthesis in HEK-293 transfectants with cycloheximide. This resulted in a markedly reduced LPL staining in intracellular vesicles after 2 hours (Fig. 5A, upper row). After 3 hours vesicular LPL was almost absent, showing that vesicular-located LPL is either secreted or degraded within 3 hours. When cycloheximide was added to the cells together with the lysosomal proteinase inhibitors leupeptin and pepstatin, vesicular staining was still present even after 6 hours (Fig. 5A, lower row). Although

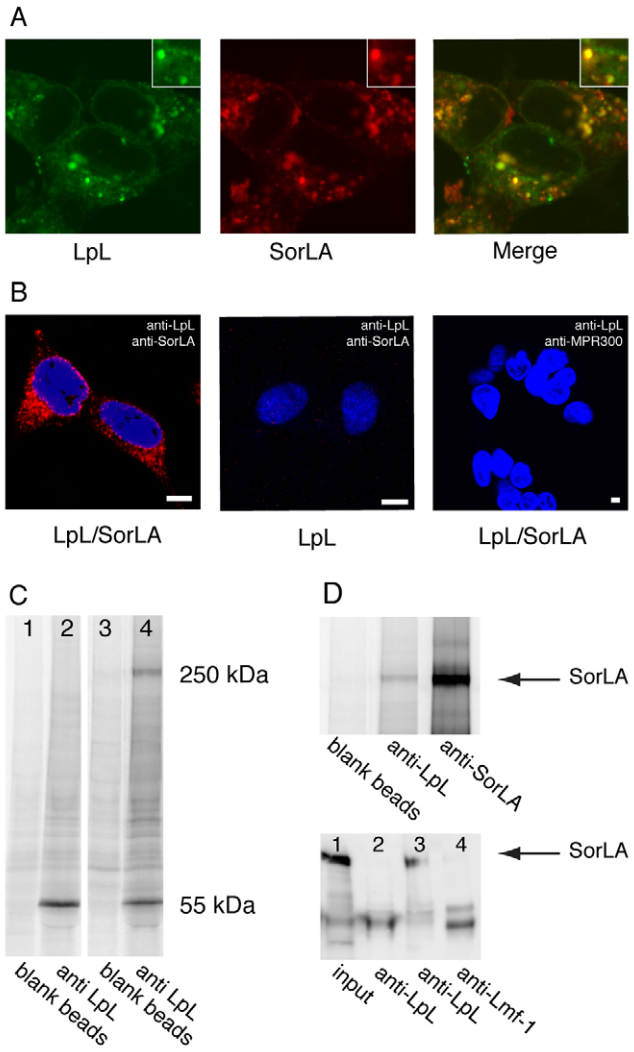

Fig. 4. Cellular binding of LPL to SorLA. (**A**) HEK-293 cells coexpressing LPL and SorLA (LpL/SorLA), stained with rabbit anti-SorLA and mouse anti-LPL antibodies, indicates a large degree of colocalization between SorLA and LPL. As secondary antibodies, goat anti-(mouse Ig) and goat-anti-(rabbit Ig) antibodies, conjugated to Alexa-Fluor-488 and Alexa-Fluor-568, respectively, were used. The insets show a magnified region with colocalization. (**B**) Duolink in situ proximity ligation assay (PLA) performed on LPL and SorLA coexpressing and LPL-expressing cells. Chicken anti-LPL and mouse anti-SorLA antibodies were used as primary antibodies, and as secondary plus and minus probes we used PLA–anti-(mouse Ig) and PLA–anti-(chicken Ig), respectively. Positive reactions were detected with a 563-nm-fluorescence-label detection kit. As a control, mouse-anti-LPL and rabbit-anti-MPR300 were used as primary antibodies. (**C**) LPL (55 kDa) from the crosslinked lysates of biolabelled HEK-293 LPL-expressing (lanes 1 and 2) and LpL/SorLA cells (lane 3 and 4) was precipitated with a polyclonal anti-LPL antibody or blank beads. In cells coexpressing SorLA (250 kDa), the receptor was co-precipitated. (**D**) Upper panel: SorLA from the crosslinked lysates of biolabeled LpL/SorLA cells was precipitated with rabbit-anti-LPL, rabbit-anti-SorLA or blank beads to verify that the precipitated 250 kDa band represents SorLA. Lower panel: western blot, probed with rabbit-anti-SorLA antibody, of cross-linked LPL and LpL/SorLA transfectants. Lane 1, crude LpL/SorLA cell lysate (input); lane 2, LPL transfectants, cross-linked with DSP and immunoprecipitated with mouse-anti-LPL; lane 3, LpL/SorLA transfectants, crosslinked with DSP and immunoprecipitated with mouse-anti-LPL antibody; lane 4, LpL/SorLA transfectants, cross-linked with DSP and immunoprecipitated with rabbit-anti-LMF1 antibody. Scale bars: 5 µm.

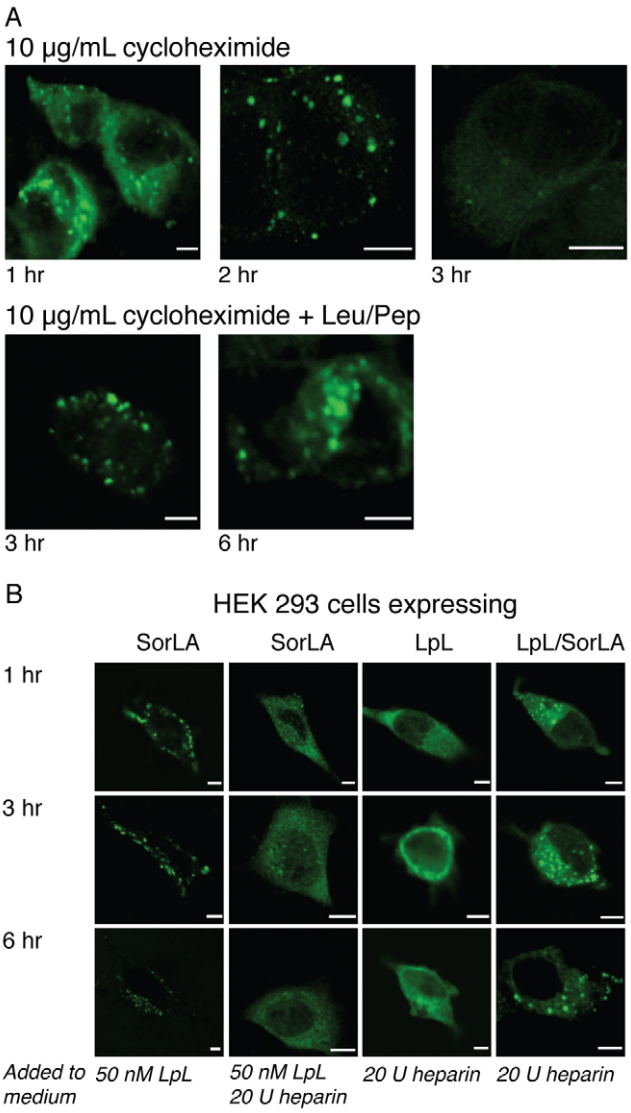

Fig. 5. Sorting of LPL in HEK-293 cells. HEK-293 cells expressing LPL, SorLA or both (LpL/SorA) were treated with cycloheximide, leupeptin and pepstatin (Leu/Pep) and/or heparin, as indicated. After incubation, the cells were fixed and stained with mouse anti-LPL antibody. (**A**) Upper panel: blocking protein synthesis with cycloheximide demonstrates that the lifetime of vesicular LPL is less than 3 hours. Lower panel: cycloheximide used together with cellular proteinase inhibitors prolongs the lifetime of vesicular LPL to more than 6 hours. (**B**) Blocking endocytosis of LPL with heparin shows that vesicular LPL is observed over the whole incubation period, indicating that newly synthesized LPL is transported directly to vesicles. Scale bars: 5 µm.

there was very little LPL staining after 3 hours in the presence of cycloheximide, we wanted to exclude the possibility that LPL is simply secreted and then subsequently re-endocytosed to endosomes. It has been demonstrated and widely accepted that LPL undergoes receptor-mediated endocytosis and that heparin blocks this uptake by releasing LPL from the cell surface. Accordingly, we also found that exogenous LPL is endocytosed in HEK-293 cells expressing SorLA, and that this uptake is blocked by heparin (Fig. 5B, columns 1 and 2). The weak surface staining that is observed in the presence of heparin probably represents a

fraction of monomerized LPL, which is known to be insensitive to heparin (Makoveichuk et al., 2004). Column 3 in Fig. 5B shows that heparin itself does not induce vesicular LPL staining of endogenously expressed LPL. As endosomes are depleted for LPL after 3 hours when protein synthesis and LPL uptake are blocked, we concluded that the LPL-positive endosomes seen after 6 hours must be due to a direct transport of newly synthesized LPL from the TGN, as uptake from the cell surface was blocked by heparin (Fig. 5B, column 4).

SorLA increases the turnover of LPL

Ligands that are transported to EEs are often sent to lysosomes for degradation. Intra- and extra-cellular LPL enzyme activities (triacylglycerol hydrolysis, see the Material and Methods section) and protein concentrations were therefore measured in order to examine whether SorLA-mediated sorting was accompanied by a change in the turnover of LPL. Compared with LPL-expressing cells, double transfectants reduced the extracellular LPL activity by 67% and the intracellular LPL activity by 83% (Fig. 6). As the reduction in the total mass of LPL followed enzyme activity (data not shown), the decreased LPL activity must have been a result of LPL degradation and not inactivation. By contrast, transfection with the sorting-impaired SorLA-ΔMVIA variant causes a measurable reduction in the anterograde transport of SorLA to endosomes (Nielsen et al., 2007). Coexpressing SorLA-ΔMVIA with LPL did not significantly affect turnover of LPL (Fig. 6). This observation supports the idea that SorLA transports LPL directly from the TGN to endosomes. Likewise, sortilin, which carries a propeptide that inhibits binding of ligands in Golgi, did not influence the overall LPL enzyme activity.

To visualize whether LPL finally ends up in the acidic lysosomes, double-labeling of LPL and the lysosomal marker LAMP1 was performed in LPL and SorLA coexpressing cells. As judged by the amount of colocalized LPL and LAMP1, an increased amount of LPL appeared in lysosomes when cells were treated with the proteinase inhibitors leupeptin and pepstatin (Fig. 7A, lower row). The presence of leupeptin and pepstatin also increased the amount of intracellular LPL activity in LPL and SorLA coexpressing cells by 91%, whereas LPL activity in cells without SorLA was only increased by 19% (Fig. 7B).

Similar results were obtained with biolabeled LPL in LPL-expressing and LPL and SorLA coexpressing cells (Fig. 7C). Cells were pulsed for 3 hours with radioactive amino acids and chased for 0, 2 or 4 hours. The experiments were performed in the presence of heparin to block re-uptake of secreted LPL. Precipitation of labeled LPL revealed a faster degradation of intracellular LPL in the presence of coexpressed SorLA (Fig. 7C). In three independent experiments, the amount of non-degraded LPL in LPL-transfected cells was quantified as 52.7% (s.e.m.±8.1) and 23.0% (s.e.m.±9.18) after 2 and 4 hours, respectively. At the same time points these numbers were, respectively, 23.15% (s.e.m.±9.8) and 5.83% (s.e.m.±1.12) in SorLA cotransfectants. Keeping in mind that all clones have similar levels of *LPL* mRNA (Table 1), these data indicate an increased SorLA-mediated turnover of LPL.

SorLA sorts LPL to distinct vesicles in neurons and glia cells

In addition to adipose tissue and muscle, LPL expression is also detected in neurons and glia cells of the brain, with the highest levels found in the hippocampus (Xian et al., 2009). As SorLA is highly expressed throughout the brain, we speculated that SorLA might play an important role in the regulation of LPL activity in this tissue. Thus, to compare the subcellular localization of LPL and SorLA in the hippocampus, we generated synaptosomal preparations of mouse hippocampus. LPL and SorLA were mainly found outside the synaptosomes, suggesting that both proteins are mainly found in the cell soma (Fig. 8A). By analogy, LPL staining was observed in distinct vesicle-like structures in the soma of primary hippocampal neurons (Fig. 8B,C) and occasionally in neurites (data not shown). Similar staining was seen in cultures of cortical glia cells (Fig. 8D). Importantly, such punctate LPL staining was absent in neurons and glia prepared from *SorLA*-knockout mice. Instead, LPL staining was diffuse and distributed throughout the cytoplasm, in a manner similar to that described above for transfected HEK-293 cells (Fig. 8C,D and Fig. 2B). This clearly shows that SorLA regulates LPL trafficking in these cell types, and suggests that SorLA is crucial for LPL subcellular localization in the central nervous system.

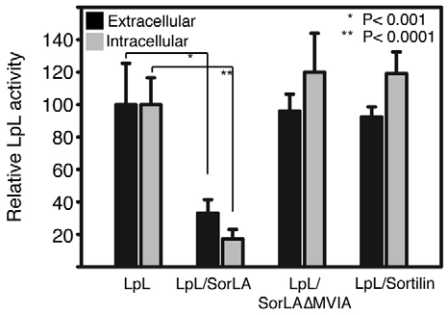

Fig. 6. The effect of SorLA on cellular LPL activity. Intracellular and extracellular LPL activity in HEK-293 cells expressing LPL with and without SorLA, SorLA-ΔMVIA or sortilin. Each bar represents at least three measurements from three individual experiments, and LPL enzyme activities in all four samples were normalized to the intracellular and extracellular LPL activity in LPL transfectants (set to 100%; extracellular and intracellular activities were equal to 43.39 milliunits/ml and 129.9 milliunits/ml, respectively).

Discussion

Sortilin and SorLA bind many of the same ligands that also bind the LDL receptors. Although LDL receptors are primarily located on the cell surface, where they participate in cell signaling and facilitate the uptake of ligands, sortilin and SorLA are mainly intracellular, and partake in sorting between the TGN and endosomes (May et al., 2005; Nielsen et al., 2007; Nielsen et al., 2001). Newly synthesized sortilin and SorLA cannot bind ligands to their Vps10p-D until they have passed through the TGN, where the propeptide is released through cleavage with furin (Munck Petersen et al., 1999). Although LPL binds to the Vps10p-D in sortilin, we demonstrate here that the LPL-binding domain in SorLA is placed in the LA repeats. As the LA repeats in SorLA are not blocked by the propeptide, it is possible for LPL to bind to SorLA in the early compartments of the biosynthetic pathway, such as in the Golgi and TGN. Even under the slightly acidic conditions in the TGN and endosomes, binding between LPL and SorLA is still possible.

On the basis of these observations we wanted to determine whether SorLA could interfere with LPL transport in cellular systems. We observed an increasing accumulation of LPL in vesicular structures, when LPL was coexpressed with SorLA.

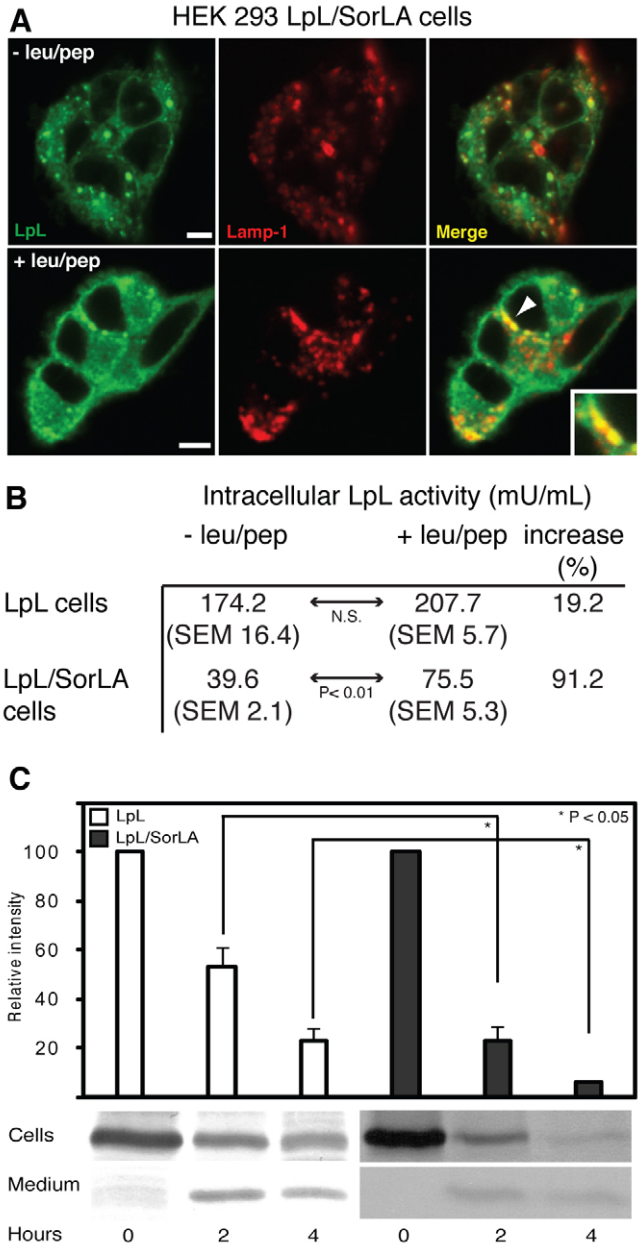

Fig. 7. Degradation of LPL. (**A**) HEK-293 LPL and SorLA coexpressing cells (LpL/SorLA) were treated with leupeptin and pepstatin (+ leu/pep) for 24 hours (medium replaced every 6 hours) and compared with untreated cells. After fixation, the cells were stained with chicken anti-LPL (green) and mouse anti-LAMP1 (a lysosomal marker; red) as primary antibodies. (**B**) Intracellular LPL activity in HEK-293 cells measured with and without leupeptin and pepstatin in cells expressing LPL and/or SorLA. The values are LPL enzyme activity given in milliunits per ml of total cell extract with a protein concentration of 1.3 mg/ml. (**C**) Cells were biolabeled in the presence of brefeldin A and chased for 0, 2 or 4 hours. Labeled LPL was then precipitated from the medium and lysates with polyclonal rabbit anti-LPL antibody, and analyzed by reducing SDS-PAGE and autoradiography. The intensity of the cellular fractions (average of several experiments) is shown in the histogram. Error bars show the s.e.m. Scale bars: 5 µm.

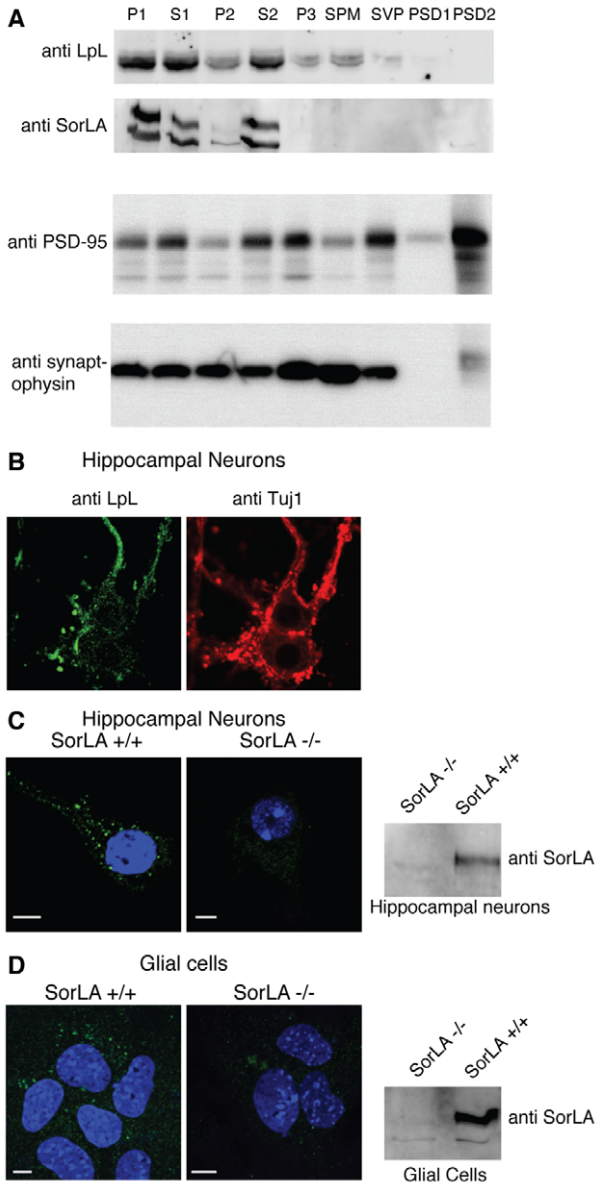

Fig. 8. SorLA regulates LPL trafficking in the central nervous system. (**A**) Synaptosomal preparations of mouse hippocampus, analyzed by western blotting, showing that the majority of SorLA and LPL is localized close to the soma of hippocampal neurons and outside of synaptosomes. Fractions were also probed using antibodies against the synaptic markers synaptophysin and PSD-95, and the purity of postsynaptic densities was validated by the absence of synaptophysin and the presence of PSD-95. P1 and S1, initial pellet and supernatant, respectively; P2, a crude synaptosomal preparation; S2, light membrane fraction; P3, synaptosomal membrane fraction; SPM, synaptic plasma membrane; SVP, synaptic vesicle preparation; PSD, postsynaptic densities. (**B**) Primary cultures of hippocampal neurons prepared from wild-type mice were stained using antibodies against LPL (green) and the neuron-specific marker Tuj1 (red). (**C**) Hippocampal neurons prepared from wild-type (+/+) and *SorLA*-knockout mice (–/–) were stained for LPL (green). Nuclei were visualized using DAPI (blue). (**D**) Similar staining of primary cortical glia cells. Both cell types have a high endogenous expression of SorLA, as shown by western blotting (gels on the right-hand side).

Using the scan^R screening system we found approximately twice as many LPL-positive vesicles in cells coexpressing SorLA. The effect of SorLA on the intracellular localization of LPL was also evident when cellular vesicles were separated by use of ultracentrifugation. The effect was most clear when LPL was expressed with a variant of SorLA that lacks the last four amino

acids in the cytoplasmic domain (SorLA-ΔMVIA). From previous work, we know that this variant of SorLA shuttles substantially less between the TGN and MVB/LEs, because MVIA is important for binding to the cytosolic adaptors GGA1, 2 and 3. Electron microscope images of SorLA demonstrate the presence of SorLA in EEs, MVB/LEs and electron-dense tubules or vesicles preferentially surrounding the EEs. Similar tubular endosomal structures surrounding the EEs have previously been demonstrated to be an endosome-to-TGN recycling compartment for sortilin and MPR300 (Mari et al., 2008). This recycling was suggested to involve SNX1, which is a subunit of the retromer complex and which is also located in the recycling compartment. As we know that SorLA is transported in an SNX1-dependent manner back to the TGN (Nielsen et al., 2007), it is tempting to speculate that the SorLA-positive electron-dense tubules also function as endosome-to-TGN recycling compartments for SorLA. Fluorescent double-labeling of LPL and SorLA, and the PLA, demonstrated a tight colocalization between LPL and SorLA. Moreover, using an intracellular crosslinker, coimmunoprecipitation of SorLA with LPL was demonstrated. We therefore conclude that intracellular LPL is located in close proximity to SorLA and that a physical interaction is likely to take place.

As SorLA internalizes ligands and also facilitates anterograde transport from TGN to endosomes, the increased amount of LPL-positive peripheral punctated structures could result from either transport route. In our experiments, the lifetime for LPL in these punctated structures, which probably correspond to endosomes, was less than 3 hours. Furthermore, when blocking receptor-mediated endocytosis for up to 6 hours, LPL-positive vesicle-like structures were still observed. Thus, we believe that a fraction of newly synthesized LPL is transported directly from the TGN to the endosomal system. This is the first time it has been demonstrated that SorLA can bring cargo by way of anterograde transport from the TGN to the endosomal system (Fig. 9).

To evaluate the consequences of this SorLA-mediated intracellular transport, we measured LPL activity in cells with and without SorLA and sortilin. The experiment showed that intracellular LPL activity and mass was reduced ~80% in cells coexpressing SorLA. As the *LPL* mRNA level was not affected by clonal selection, we infer that SorLA mediates LPL degradation. Furthermore, coexpressing LPL with the MVIA-deleted SorLA receptor restored the LPL activity levels similar to those found in cells without wild-type SorLA. As the MVIA motif only influences the cellular TGN-to-endosome transport, and not the endocytosis, this finding supports the conclusion that SorLA transports LPL directly from the TGN to endosomes. We assumed that the increased degradation of LPL took place in the lysosomes, and therefore we repeated the activity measurements in the presence of the proteinase inhibitors leupeptin and pepstatin. In this setup, intracellular LPL activity in the SorLA cells was increased by over 90% compared with less than 20% in cells expressing only LPL. Furthermore, LPL colocalized with the lysosomal marker LAMP1 in the presence of lysosomal proteinase inhibitors. We therefore conclude that SorLA enhances the degradation of LPL by routing it to lysosomes.

LPL is regulated in a tissue-specific manner, and the regulation takes place on every step from transcriptional to post-transcriptional levels (Wang and Eckel, 2009). The first step in the post-transcriptional regulation is in the ER, where LMF1 tightly regulates the activation of LPL (Fig. 9). LMF1 is ubiquitously expressed, and lack of functional LMF1 results in severe hypertriglyceridemia (Peterfy et al., 2007). Here, we demonstrate that SorLA might be

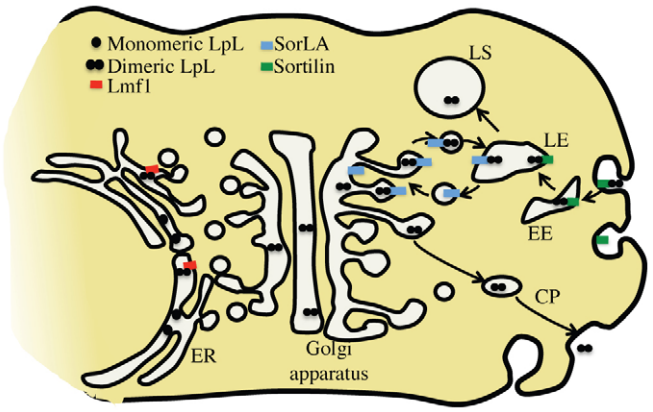

Fig. 9 Model of LPL trafficking. LPL achieves its dimeric active form in the ER through an LMF1-dependent process. After passage through the Golgi, LPL can be secreted by the constitutive pathway (CP) or it can bind to SorLA in the TGN and be sorted to late endosomes (LEs). From the LEs, SorLA returns to the TGN, and LPL continues to lysosomes (LS). Sortilin (and receptors of the LDL receptor family) can facilitate receptor-mediated uptake of secreted LPL, whereby LPL also ends up in lysosomes for degradation.

an important post-transcriptional regulator of LPL in the TGN. However, SorLA is only expressed in a subset of LPL-producing cells, and we therefore suspect that SorLA is one of the proteins involved in tissue-specific LPL regulation. Both SorLA and LPL are highly expressed in the hippocampus, and our synaptosomal preparations of hippocampi from wild-type mice suggest that the majority of SorLA and LPL are localized in the soma of neurons. The presence of LPL in the cell soma was confirmed in primary hippocampal neurons and cortical glia cells by using immunofluorescence, showing that LPL was localized in distinct vesicle-like structures. Of particular importance was the finding that no such punctate LPL staining was observed in cultures prepared from *SORL1*-knockout mice. Taken together, our findings demonstrate that SorLA plays a crucial role for LPL trafficking in cells of the central nervous system. Interestingly, we observed that a minor fraction of LPL was found in presynaptic vesicles but that it was absent from postsynaptic densities. LPL-deficient mice display impaired memory and this phenotype is attributed to a presynaptic defect in the hippocampus (Xian et al., 2009). Hence, it is tempting to speculate that SorLA regulates the routing of LPL to presynaptic vesicles and thereby affects general cognition. Other evidence indicates that LPL is involved in the distribution of cholesterol and other lipids in the brain. The need for lipids after an injury fits with the observation of Paradis et al. (Paradis et al., 2004), who demonstrate that LPL is upregulated after ischemia.

In this study, we have demonstrated that SorLA can transport LPL directly from the biosynthetic pathway to the endosomal system, from which LPL is forwarded to lysosomes (Fig. 9). This is the first time a direct intracellular transport mechanism from the early biosynthetic system has been demonstrated for SorLA. We have also shown that the Vps10p-D receptor sortilin cannot act as an intracellular-sorting receptor for LPL in the early compartments of the biosynthetic pathway, because the Vps10p-D is blocked by the propeptide. This finding contributes to the understanding of the complex trafficking and regulation of LPL in the brain, where altered LPL levels are observed in relation to cerebral strokes and Alzheimer's disease.

Materials and Methods

Surface plasmon resonance

The soluble domains of SorLA and sortilin and the Vps10p domain of SorLA were purified from stably transfected CHO cells, as described previously (Jacobsen et al., 2001; Tauris et al., 1998). Bovine LPL was purified from bovine milk on a heparin column (Bengtsson-Olivecrona and Olivecrona, 1991). Measurements were performed on a BIAcore 3000 instrument and kinetic parameters were determined using the BIAevaluation 4.1 software. The BIAcore 3000 instrument was equipped with CM5 sensor chips maintained at 4°C. The sensor chip was activated by injection of 0.2 M *N*-ethyl-*N*-(3-dimethylaminopropyl)carbodiimide and 0.05 M *N*-hydroxy-succinimide in water. A 10 mM sodium acetate solution of 15–35 μg/ml purified receptor was injected over flow cells 2–4, giving densities of 88 fmol/mm^2, 64 fmol/mm^2 and 23 fmol/mm^2 for sortilin, SorLA and Vps10p-SorLA, respectively. Remaining binding sites were blocked with 1 M ethanolamine. Flow cell 1 was activated and blocked without protein and used as a reference. The samples were injected in 10 mM HEPES pH 7.4, 150 mM NaCl, 1.5 mM $CaCl_2$, 1 mM EGTA and 0.010% surfactant P20, and this was also used as the running buffer. To obtain the relative response units, the response from flow cell 1 was subtracted from the responses from flow cells 2–4. The sensor chip was regenerated by injection of 10 mM glycin pH 4.0, 20 mM EDTA, 500 mM NaCl and 0.005% surfactant P20.

DNA and cell cultures

SorLA (GenBank accession number NM_003105) and sortilin (GenBank accession number NM_002959) full-length constructs were made as described previously (Nielsen et al., 2007). Human LPL (GenBank accession number NM_000237) was cloned into the pcDNA5/FRT/Hyg vector (Invitrogen). HEK-293 Flp-In cells (Invitrogen) were transfected with the pcDNA5/FRT/Hyg construct, containing full-length LPL, together with the pOG44 vector. Cells were transfected using FuGENE 6 transfection reagent (Roche), and stably transfected clones were selected with 500 μg/ml hygromycin. Clones were selected for further stable transfection with pcDNA3.1(–)zeo constructs containing full-length or mutant SorLA, or full-length sortilin. For selection, clones were cultured with 500 μg/ml zeocin and 500 μg/ml hygromycin.

Cortical glia cells were prepared from P0 (postnatal day 0) pups. In brief, isolated cortex was digested with papain (Worthington, Lakewood, NJ) followed by treatment with 100 μg/ml DNaseI (Sigma). Then the tissue was triturated in Dulbecco's modified Eagle's medium (DMEM) containing 10% fetal bovine serum (FBS) and 0.1 mg/ml primocin (Amaxa; Lonza Cologne, Germany), and seeded onto laminin-coated coverslips. After 2 hours in the incubator, cold medium (4°C) was added in order to kill the neurons and leave only glia cells. Hippocampal neurons were prepared similarly from isolated P0 hippocampus and cultured in neurobasal medium (Gibco, Invitrogen) supplemented with Glutamax, 2% B27 supplement (Invitrogen), 20 μM 5-fluorodeoxyuridine (Sigma) and 0.1 mg/ml primocin.

qRT-PCR

cDNA was generated from quadruplicates (n=4) of each cell type using a FastLane Cell cDNA Kit and a mixture of oligo-dT and random hexamers (Qiagen). qRT-PCR was performed in a 96-well format using a LightCycler 480 instrument (Roche) and the SYBR green method, according to the manufacturer's instructions (Roche). PCR primer pairs are listed in supplementary material Table S1. For all primer pairs, the amplification efficiency was determined from a serial dilution and found to be above 95%. Samples were analyzed in triplicates and the mean expression levels, corresponding to *SORL1* and *LPL* mRNA expression were normalized to *HPRT1* (an endogenous housekeeping gene) mRNA levels using the Genex software (http://www.multid.se). Controls without reverse transcriptase for all cell-types showed no amplification, demonstrating no genomic DNA contamination in the RNA samples.

Immunofluorescence

Cells growing on coverslips were fixed in 4% formaldehyde and permeabilized in 0.5% saponin. For secondary labeling, Alexa-Fluor-488 and -568-conjugated antibodies (Invitrogen) were used. Cells were analyzed using an LSM510-META laser-scanning confocal microscope using a 40 or 63× C-Apochromat water immersion objective, NA 1.2 (Carl Zeiss, Göttingen, Germany). For inhibition of lysosomal hydrolases, 50 μg/ml leupeptin and pepstatin (Sigma) were added (and replaced every 6 hours) to the medium at 24 hours before fixation.

High-content imaging and quantitative analysis was performed with the Olympus scan^R imaging station. Images were acquired with a 40× objective, a triple-band emission filter for Hoechst 33258, Alexa-Fluor-488 and Alexa-Fluor-568, and a Hamamatsu camera (C8484-05G). For image analysis, *z*-stack-projected images were background-subtracted, after which an edge-detection algorithm was used for segmentation of nuclei and LPL-containing vesicles. Vesicles were detected using this algorithm, which makes use of the gradient of the intensity in the image. If a closed connecting line (edge) can be drawn around an object, the object is segmented. Objects were recognized and selected, independent of their shape, with the only limitation that they should be smaller than 3 μm in diameter. About 95% of the detected objects were smaller than 1 μm in diameter and the average diameter of the detected vesicles was ~500 nm. After gating out the images with zero cells or with imaging artifacts, the mean number of LPL vesicles per cell was determined by calculating for each image the ratio of vesicles to nuclei.

The antibody against LPL was from the egg yolk of chickens immunized with bovine LPL, mouse anti-LPL and rabbit anti-LAMP1 antibodies were generous gifts from John D. Brunzell and Sven Carlsson. Rabbit anti-LPL, mouse anti-SorLA and rabbit anti-SorLA antibodies were produced in-house. Anti-TGN46 antibody was from AbD Serotec (Hamar, Norway) and anti-LMF1 antibody was from Sigma.

Subcellular fractionation

For preparation of a post-nuclear supernatant (PNS), HEK-293 Flp-In cells were washed in Tris-buffered saline (TBS) and harvested in TBS with 0.4 mM PMSF at 583 ***g*** for 10 minutes. The cells were resuspended in 10 ml of homogenization buffer (0.25 M sucrose, 1 mM EDTA, 1 mM magnesium acetate, 0.4 mM PMSF and 10 mM HEPES-KOH pH 7.2) and centrifuged at 583 ***g*** for 7 minutes. The cells were resuspended in 700 μl of homogenization buffer and disrupted by seven passages though a 21-gauge needle followed by five passages through a steel cell cracker (EMBL, Heidelberg, Germany) with a 9-μm gap. The PNS was obtained after removal of nuclei and unbroken cells by centrifugation at 1843 ***g*** for 7 minutes.

For subcellular fractionation, the PNS was subjected to density-gradient centrifugation (SW41Ti rotor, 25,000 rpm, for 18 minutes) on a linear 0.3–1.2 M sucrose gradient prepared by mixing at angles of 45° for 10 minutes and at 80° for 1 minute using a BioComp gradient master (BioComp, Fredericton, Canada). Fractions of 1 ml were collected from the top using a BioComp piston gradient fractionator. Selected fractions were pooled and subjected to equilibrium-gradient centrifugation on a 0.8–1.2 M non-linear sucrose gradient with 5% increments (SW41Ti rotor, 25,000 rpm, overnight). Fractions were collected and analyzed by western blotting.

Electron microscopy

HEK-293 SorLA-expressing cells, grown to 80% confluence, were fixed by adding freshly prepared 4% formaldehyde in 0.1 M phosphate buffer (pH 7.4) to an equal volume of culture medium for 10 minutes, followed by post-fixation in 4% formaldehyde at 4°C overnight. Ultrathin cryosectioning and immuno-gold labeling was performed as previously described (Liou et al., 1996; Slot et al., 1991).

Proximity ligation assay

The proximity ligation assay (PLA) has been described in detail previously (Soderberg et al., 2006). Briefly, cells were fixed with 4% formaldehyde for 20 minutes, permeabilized with 0.5% saponin and incubated with chicken anti-LPL plus mouse anti-SorLA antibodies, or mouse anti-LPL plus rabbit anti-SorLA antibodies for 90 minutes. As secondary antibodies, conjugated with oligonucleotides, we used PLA(+)–anti-(chicken Ig) plus PLA(–)–anti-(mouse Ig), and PLA(–)–anti-(mouse Ig) plus PLA(+)–anti-(rabbit Ig), respectively. After hybridization and ligation, interacting probes were amplified with polymerase. Finally, a 563-nm-fluorescence-label detection kit (source??) was used to detect interactions. All incubations were performed at 37°C, using the incubation times and buffers given in the manufacturer's instructions (Olink Bioscience, Uppsala, Sweden).

Metabolic labeling, affinity precipitation and crosslinking

Transfected HEK-293 Flp-In cells were cultured in poly-L-lysine-coated six-well trays (Sigma) to ~60% confluence. The cells were washed twice and preincubated for 20 minutes in cysteine- and methionine-free modified Eagle's medium (Sigma) with 2% dialyzed FBS. Biolabeling was performed in the same medium supplemented with 10 μg/ml brefeldin A (Sigma) using 11.1 MBq/ml [^{35}S]L-cysteine and [^{35}S]L-methionine (pro-mix, GE Healthcare) for 3 hours at 37°C. For chase experiments, the cells were washed twice and incubated in complete DMEM with 20 units/ml heparin for 2–4 hours before the medium was harvested. Alternatively, the medium was harvested immediately after the labeling period. The cells were washed with PBS (4°C) and subsequently lyzed for 10 minutes in 1% Triton X-100 (in 20 mM Tris-HCl, pH 8.0, 10 mM EDTA and 150 mM NaCl).

For immunoprecipitation, the cell lysates and medium (1 ml) were preincubated with 50 μl of uncoupled CNBr-activated Sepharose 4B beads (GE Healthcare) (for 2 hours at 4°C) before incubation with 75 μl of GammaBind-G–Sepharose beads (GE Healthcare) coated with a rabbit polyclonal anti-LPL antibody (2 h, 4°C). The beads were washed five times in PBS pH 7.4 with 0.05% Tween 20, and prepared for SDS-PAGE by boiling for 3 minutes in 100 μl of reducing sample buffer (10 mM dithiothreitol and 2.5% SDS).

For crosslinking, labeled cells were washed with PBS and incubated for 30 minutes with 2 mM DSP (Thermo Scientific) at room temperature, after which 100 mM Tris-HCl, pH 7.5, was added for 15 minutes. Cells were washed in twice in PBS and lysed for 10 minutes as described above. Immunoprecipitation was afterwards performed with various antibodies.

LPL sorting

HEK-293 Flp-In cells expressing LPL and SorLA were incubated for 1, 3 and 6 hours in medium containing 20 units of heparin (SAD, Copenhagen, Denmark), for 3 and 6 hours in medium containing 10 μg/ml cycloheximide and 50 μg/ml leupeptin and pepstatin, or for 1, 2 and 3 hours in medium with 10 μg/ml cycloheximide only.

The sorting of LPL was tested with HEK-293 cells expressing SorLA, LPL or both. The cells were incubated for 1, 3 and 6 hours in medium containing 50 nM LPL and/or 20 units heparin. Owing to the half-life of LPL and heparin, the medium was replaced every 3 hours.

LPL activity measurements

Samples were incubated with 200 µl of a medium containing a phospholipid-stabilized emulsion of soybean triacylglycerols, with the same composition as Intralipid, into which ^{3}H-labeled triolein had been incorporated by sonication (Fresenius-KABI, Uppsala, Sweden). The medium also contained 6% BSA, 16 units/ml of heparin, to stabilize the lipase, 5% PMSF-treated heat-inactivated frozen rat serum, as a source of apoCII, 0.1 M NaCl and 0.15 M Tris-HCl, pH 8.5. Incubations were performed in a water-bath at 25°C and exact time was noted. The reactions were stopped by addition of 2 ml of an isopropanol, heptane and sulfuric acid mixture (40:48:3.1), with 0.5 ml water. After vortexing and centrifugation, the upper heptane phase was transferred into a new tube containing alkaline-ethanol. Heptane was added followed by vortexing and centrifugation. The upper phase was removed and the step repeated. Finally, the amount of labeled fatty acids in the lower phase was measured in a scintillation counter (WinSpectra, Wallac, Germany). Samples were assayed in triplicates. The activity was corrected for variations in the amount of cells by measuring the protein concentration of the lysates. One milliunit of lipase activity corresponds to the release of 1 nmol of fatty acids per minute.

Hippocampal synaptosomal preparations

The procedure for fractionation of hippocampi from wild-type mice into synaptosomes, synaptic vesicle fractions, synaptic plasma membrane and postsynaptic densities was performed essentially as described previously (Blackstone et al., 1992). Briefly, the hippocampus was isolated from the brains of 12 wild-type mice (8–12 weeks of age) and homogenized in 0.32 M sucrose and 4 mM HEPES pH 7.4, containing proteinase inhibitors. P1 and S1 are the pellet and supernatant, respectively, after centrifugation for 10 minutes at 1000 ***g***. S1 was further centrifuged for 15 minutes at 10,000 ***g*** to obtain supernatant S2 and pellet P2, a crude synaptosomal preparation. Solubilized P2 was centrifuged for 15 minutes at 10,000 ***g*** and the resulting pellet was solubilized in ice-cold water and centrifuged again at 25,000 ***g*** for 20 minutes, generating the synaptosomal membrane fraction P3. The supernatant was further centrifuged at 165,000 ***g*** for 2 hours generating pellet SVP, enriched in presynaptic vesicles. Solubilized P3 was applied to a discontinuous gradient containing 0.8, 1.0, and 1.2 M sucrose and centrifuged at 150,000 ***g*** for 2 hours. The fraction between the 1.0 and 1.2 M sucrose layer was recovered and diluted to give 0.32 M sucrose, after which it was centrifuged again at 150,000 ***g*** for 30 min., resulting in pellet SPM, containing the synaptic plasma membrane. Resuspended SPM was centrifuged at 35,000 ***g*** for 20 minutes to obtain the pellet PSDI, containing postsynaptic densities. This pellet was again solubilized and centrifuged at 200,000 ***g*** for 20 minutes, to obtain the concentrated postsynaptic-density fraction PSDII. All centrifugation steps were performed at 4°C. Total protein concentration in fractions was determined using a bicinchoninic acid kit (Sigma), and equal amounts of proteins of each fraction were separated by reducing SDS-PAGE and analyzed by western blotting.

Use of animals

Housing, breeding and experimentation with mice complied with approved standards for humane treatment of vertebrate animals (Ministry of Justice, Denmark: permission number J.2006/561-1206).

We thank Inger Andersen (Department of Medicinal Biochemistry, Aarhus, Denmark), Marc van Peski (Department of Cell Biology, Utrecht, The Netherlands) and Solveig Nilsson (Department of Medical Biosciences, Umeå, Sweden) for technical assistance. The MIND-center is sponsored by The Lundbeck Foundation and support was also obtained from the Swedish Research Council (grant no 12203). The use of the Normic-UIO imaging platform at the Department of Molecular Biosciences, University of Oslo is acknowledged. G.K. was supported by grants from the Norwegian Research Council.

Supplementary material available online at
http://jcs.biologists.org/cgi/content/full/124/7/1095/DC1

References

Andersen, O. M., Reiche, J., Schmidt, V., Gotthardt, M., Spoelgen, R., Behlke, J., von Arnim, C. A., Breiderhoff, T., Jansen, P., Wu, X. et al. (2005). Neuronal sorting protein-related receptor sorLA/LR11 regulates processing of the amyloid precursor protein. *Proc. Natl. Acad. Sci. USA* **102**, 13461-13466.

Bengtsson-Olivecrona, G. and Olivecrona, T. (1991). Phospholipase activity of milk lipoprotein lipase. *Methods Enzymol.* **197**, 345-356.

Bergo, M., Wu, G., Ruge, T. and Olivecrona, T. (2002). Down-regulation of adipose tissue lipoprotein lipase during fasting requires that a gene, separate from the lipase gene, is switched on. *J. Biol. Chem.* **277**, 11927-11932.

Blackstone, C. D., Moss, S. J., Martin, L. J., Levey, A. I., Price, D. L. and Huganir, R. L. (1992). Biochemical characterization and localization of a non-N-methyl-D-aspartate glutamate receptor in rat brain. *J. Neurochem.* **58**, 1118-1126.

Blain, J. F., Paradis, E., Gaudreault, S. B., Champagne, D., Richard, D. and Poirier, J. (2004). A role for lipoprotein lipase during synaptic remodeling in the adult mouse brain. *Neurobiol. Dis.* **15**, 510-519.

Braun, J. E. and Severson, D. L. (1992). Regulation of the synthesis, processing and translocation of lipoprotein lipase. *Biochem. J.* **287**, 337-347.

Cupp, M., Bensadoun, A. and Melford, K. (1987). Heparin decreases the degradation rate of lipoprotein lipase in adipocytes. *J. Biol. Chem.* **262**, 6383-6388.

Gliemann, J., Hermey, G., Nykjaer, A., Petersen, C. M., Jacobsen, C. and Andreasen, P. A. (2004). The mosaic receptor sorLA/LR11 binds components of the plasminogen-activating system and platelet-derived growth factor-BB similarly to LRP1 (low-density lipoprotein receptor-related protein), but mediates slow internalization of bound ligand. *Biochem. J.* **381**, 203-212.

Hermey, G., Plath, N., Hubner, C. A., Kuhl, D., Schaller, H. C. and Hermans-Borgmeyer, I. (2004). The three sorCS genes are differentially expressed and regulated by synaptic activity. *J. Neurochem.* **88**, 1470-1476.

Jacobsen, L., Madsen, P., Moestrup, S. K., Lund, A. H., Tommerup, N., Nykjaer, A., Sottrup-Jensen, L., Gliemann, J. and Petersen, C. M. (1996). Molecular characterization of a novel human hybrid-type receptor that binds the alpha2-macroglobulin receptor-associated protein. *J. Biol. Chem.* **271**, 31379-31383.

Jacobsen, L., Madsen, P., Jacobsen, C., Nielsen, M. S., Gliemann, J. and Petersen, C. M. (2001). Activation and functional characterization of the mosaic receptor SorLA/LR11. *J. Biol. Chem.* **276**, 22788-22796.

Jacobsen, L., Madsen, P., Nielsen, M. S., Geraerts, W. P., Gliemann, J., Smit, A. B. and Petersen, C. M. (2002). The sorLA cytoplasmic domain interacts with GGA1 and -2 and defines minimum requirements for GGA binding. *FEBS Lett.* **511**, 155-158.

Liou, W., Geuze, H. J. and Slot, J. W. (1996). Improving structural integrity of cryosections for immunogold labeling. *Histochem. Cell Biol.* **106**, 41-58.

Makoveichuk, E., Castel, S., Vilaro, S. and Olivecrona, G. (2004). Lipoprotein lipase-dependent binding and uptake of low density lipoproteins by THP-1 monocytes and macrophages: possible involvement of lipid rafts. *Biochim. Biophys. Acta* **1686**, 37-49.

Mari, M., Bujny, M. V., Zeuschner, D., Geerts, W. J., Griffith, J., Petersen, C. M., Cullen, P. J., Klumperman, J. and Geuze, H. J. (2008). SNX1 defines an early endosomal recycling exit for sortilin and mannose 6-phosphate receptors. *Traffic* **9**, 380-393.

May, P., Herz, J. and Bock, H. H. (2005). Molecular mechanisms of lipoprotein receptor signalling. *Cell. Mol. Life Sci.* **62**, 2325-2338.

Mazella, J., Zsurger, N., Navarro, V., Chabry, J., Kaghad, M., Caput, D., Ferrara, P., Vita, N., Gully, D., Maffrand, J. P. et al. (1998). The 100-kDa neurotensin receptor is gp95/sortilin, a non-G-protein-coupled receptor. *J. Biol. Chem.* **273**, 26273-26276.

Munck Petersen, C., Nielsen, M. S., Jacobsen, C., Tauris, J., Jacobsen, L., Gliemann, J., Moestrup, S. K. and Madsen, P. (1999). Propeptide cleavage conditions sortilin/neurotensin receptor-3 for ligand binding. *EMBO J.* **18**, 595-604.

Nielsen, M. S., Jacobsen, C., Olivecrona, G., Gliemann, J. and Petersen, C. M. (1999). Sortilin/neurotensin receptor-3 binds and mediates degradation of lipoprotein lipase. *J. Biol. Chem.* **274**, 8832-8836.

Nielsen, M. S., Madsen, P., Christensen, E. I., Nykjaer, A., Gliemann, J., Kasper, D., Pohlmann, R. and Petersen, C. M. (2001). The sortilin cytoplasmic tail conveys Golgi-endosome transport and binds the VHS domain of the GGA2 sorting protein. *EMBO J.* **20**, 2180-2190.

Nielsen, M. S., Gustafsen, C., Madsen, P., Nyengaard, J. R., Hermey, G., Bakke, O., Mari, M., Schu, P., Pohlmann, R., Dennes, A. et al. (2007). Sorting by the cytoplasmic domain of the amyloid precursor protein binding receptor SorLA. *Mol. Cell. Biol.* **27**, 6842-6851.

Nilsson, S. K., Lookene, A., Beckstead, J. A., Gliemann, J., Ryan, R. O. and Olivecrona, G. (2007). Apolipoprotein A-V interaction with members of the low density lipoprotein receptor gene family. *Biochemistry* **46**, 3896-3904.

Nilsson, S. K., Christensen, S., Raarup, M. K., Ryan, R. O., Nielsen, M. S. and Olivecrona, G. (2008). Endocytosis of apolipoprotein AV by members of the low density lipoprotein receptor and the Vps10p domain receptor families. *J. Biol. Chem.* **283**, 25920-25927.

Ohwaki, K., Bujo, H., Jiang, M., Yamazaki, H., Schneider, W. J. and Saito, Y. (2007). A secreted soluble form of LR11, specifically expressed in intimal smooth muscle cells, accelerates formation of lipid-laden macrophages. *Arterioscler. Thromb. Vasc. Biol.* **27**, 1050-1056.

Paradis, E., Clavel, S., Julien, P., Murthy, M. R., de Bilbao, F., Arsenijevic, D., Giannakopoulos, P., Vallet, P. and Richard, D. (2004). Lipoprotein lipase and endothelial lipase expression in mouse brain: regional distribution and selective induction following kainic acid-induced lesion and focal cerebral ischemia. *Neurobiol. Dis.* **15**, 312-325.

Peterfy, M., Ben-Zeev, O., Mao, H. Z., Weissglas-Volkov, D., Aouizerat, B. E., Pullinger, C. R., Frost, P. H., Kane, J. P., Malloy, M. J., Reue, K. et al. (2007). Mutations in LMF1 cause combined lipase deficiency and severe hypertriglyceridemia. *Nat. Genet.* **39**, 1483-1487.

Petersen, C. M., Nielsen, M. S., Nykjaer, A., Jacobsen, L., Tommerup, N., Rasmussen, H. H., Roigaard, H., Gliemann, J., Madsen, P. and Moestrup, S. K. (1997). Molecular identification of a novel candidate sorting receptor purified from human brain by receptor-associated protein affinity chromatography. *J. Biol. Chem.* **272**, 3599-3605.

Preiss-Landl, K., Zimmermann, R., Hammerle, G. and Zechner, R. (2002). Lipoprotein lipase: the regulation of tissue specific expression and its role in lipid and energy metabolism. *Curr. Opin. Lipidol.* **13**, 471-481.

Quistgaard, E. M., Madsen, P., Groftehauge, M. K., Nissen, P., Petersen, C. M. and Thirup, S. S. (2009). Ligands bind to Sortilin in the tunnel of a ten-bladed beta-propeller domain. *Nat. Struct. Mol. Biol.* **16**, 96-98.

Rogaeva, E., Meng, Y., Lee, J. H., Gu, Y., Kawarai, T., Zou, F., Katayama, T., Baldwin, C. T., Cheng, R., Hasegawa, H. et al. (2007). The neuronal sortilin-related receptor SORL1 is genetically associated with Alzheimer disease. *Nat. Genet.* **39**, 168-177.

Slot, J. W., Geuze, H. J., Gigengack, S., Lienhard, G. E. and James, D. E. (1991). Immuno-localization of the insulin regulatable glucose transporter in brown adipose tissue of the rat. *J. Cell Biol.* **113**, 123-135.

Soderberg, O., Gullberg, M., Jarvius, M., Ridderstrale, K., Leuchowius, K. J., Jarvius, J., Wester, K., Hydbring, P., Bahram, F., Larsson, L. G. et al. (2006). Direct observation of individual endogenous protein complexes in situ by proximity ligation. *Nat. Methods* **3**, 995-1000.

Tauris, J., Ellgaard, L., Jacobsen, C., Nielsen, M. S., Madsen, P., Thogersen, H. C., Gliemann, J., Petersen, C. M. and Moestrup, S. K. (1998). The carboxy-terminal domain of the receptor-associated protein binds to the Vps10p domain of sortilin. *FEBS Lett.* **429**, 27-30.

Vannier, C. and Ailhaud, G. (1989). Biosynthesis of lipoprotein lipase in cultured mouse adipocytes. II. Processing, subunit assembly, and intracellular transport. *J. Biol. Chem.* **264**, 13206-13216.

Wang, H. and Eckel, R. H. (2009). Lipoprotein lipase: from gene to obesity. *Am. J. Physiol. Endocrinol. Metab.* **297**, E271-E288.

Westergaard, U. B., Sorensen, E. S., Hermey, G., Nielsen, M. S., Nykjaer, A., Kirkegaard, K., Jacobsen, C., Gliemann, J., Madsen, P. and Petersen, C. M. (2004). Functional organization of the sortilin Vps10p domain. *J. Biol. Chem.* **279**, 50221-50229.

Xian, X., Liu, T., Yu, J., Wang, Y., Miao, Y., Zhang, J., Yu, Y., Ross, C., Karasinska, J. M., Hayden, M. R. et al. (2009). Presynaptic defects underlying impaired learning and memory function in lipoprotein lipase-deficient mice. *J. Neurosci.* **29**, 4681-4685.

Yamazaki, H., Bujo, H. and Saito, Y. (1997). A novel member of the LDL receptor gene family with eleven binding repeats is structurally related to neural adhesion molecules and a yeast vacuolar protein sorting receptor. *J. Atheroscler. Thromb.* **4**, 20-26.